sciendo

Polish Journal of Medical Physics and Engineering
The Journal of Polish Society of Medical Physics
ISSN 1898-0309, doi: 10.2478/pjmpe-2025-0021

September 2025
Vol 31, Issue 3

Scientific Paper

Lung diseases classification using pre-trained based deep learning model and support vector machine

Amine Ben Slama[1,ABCDEF], Yessine Amri[2,3,BCEF,*], Sabri Barbaria[1,BEF], Hanene Boussi Rahmouni[1,CEF], Hedi Trabelsi[1,ACEF]

[1]*Research Laboratory of Biophysics and Medical Technologies LRBTM (LR13ES07), Higher Institute of Medical Technologies (ISTMT), University of Tunis El Manar, Tunis, Tunisia*
[2]*Biochemistry Laboratory, Bechir Hamza Children's Hospital, Tunis, Tunisia*
[3]*Department of Educational Sciences, University of Jendouba, Higher Institute of Applied Studies in Humanity Le Kef, Le Kef, Tunisia*
**Corresponding author: Yessine Amri; amri.yessine@yahoo.com*

(received 12 June 2024; revised 2 January 2025, 19 March 2025, 30 April 2025; accepted 15 June 2025)

Abstract

Introduction: Given its rapid transmission and heightened fatality rate, early detection of viral pneumonia is imperative. The virus mainly affects the lung, leading to pneumonia alongside symptoms like fatigue, dry cough, and fever, which can sometimes be misdiagnosed as other respiratory conditions such as lung cancer or pneumonia. Chest X-rays are widely used in the healthcare sector to provide both swift and accurate diagnoses. Deep learning algorithms have demonstrated significant efficiency in detecting and classifying lung diseases, which enhanced the diagnostic process and saving valuable time for medical applications and therapy.The objective of this study is to develop and evaluate a deep learning-based architecture for the accurate multi-class classification of respiratory diseases, including pneumonia, lung opacity, and COVID-19, using chest X-ray images to enhance diagnostic efficiency in healthcare settings.

Material and methods: A substantial dataset comprising X-ray images was crated, including 1026 pneumonia cases, 1256 COVID-19 cases, 2305 lung opacity cases and 3224 normal X-ray images. For classification purposes, we employed a pre-trained VGG19 model combined with an SVM classifier. To validate the model's accuracy, we utilized cross-validation techniques and performance metrics, including precision, recall, F1-score, and the area under the curve (AUC). This approach ensures robust evaluation of the proposed framework.

Results: The experimental results demonstrated the superiority of our proposed VGG16+SVM model over existing approaches, achieving an accuracy of 93.50%, recall of 94.16%, precision of 94.45%, F1 score of 93.28%, and area under the curve (AUC) of 90.16%.

Conclusions: This enhanced performance equips healthcare practitioners with the tools to diagnose and treat patients more expeditiously and effectively.

Keywords: Pneumonia; Lung diseases; COVID-19; Deep learning; Classification.

Introduction

Different lung disease such as COVID-19, pneumonia, lung cancer primarily affect the respiratory system, leading to infection and respiratory distress, ultimately resulting in fatalities due to insufficient oxygen supply to the lungs[1]. These diseases represent a global health crisis, characterized by the high mortality rate, posing significant social, economic, and political challenges. Studies indicate an increasing frequency of pandemics over recent centuries[2].

In the medical field, computer-aided diagnosis systems have garnered attention for their potential to enhance diagnostic capabilities. Collaborations between medical researchers and computer scientists have yielded sophisticated systems capable of replicating the decision-making processes of medical professionals. These systems, often categorized as expert systems, excel in processing complex and extensive clinical data[3].

Moreover, computer-aided detection systems play a crucial role in assisting clinicians by providing valuable insights into patient data, thereby improving diagnostic accuracy. These systems are regarded as intelligent, as they incorporate feedback mechanisms to continually refine their performance[4,5]. Studies have demonstrated that some advanced models, such as those leveraging reinforcement learning or iterative updating, can refine their performance over time by integrating user feedback or adapting to new datasets leading to difficulties in

© 2025 Authors
This is an open access article licensed under the Creative Commons Attribution-NonCommercial-NoDerivs License (http://creativecommons.org/licenses/by-nc-nd/4.0/).

Authors' contribution:
A – Research concept and design, B – Collection and/or assembly of data, C – Data analysis and interpretation, D – Writing the article, E – Critical revision of the article, F – Final approval of the article.

analysis. However, analyzing large clinical datasets poses significant challenges. Intelligent computer-aided diagnosis systems, leveraging data mining, artificial intelligence (AI), and deep learning methodologies, offer promising solutions for diagnosing a wide range of medical conditions and disorders.

In recent years, advancements in medical imaging technologies such as chest X-rays,[6,7] ultrasounds, and magnetic resonance imaging (MRI) have revolutionized disease diagnosis, leading to significant improvements in healthcare and medical research. Advanced AI technology has greatly enhanced the accuracy of diagnosing various human diseases, thereby improving patients' quality of life. However, medical experts have historically faced challenges in achieving accurate diagnoses, resulting in unnecessary healthcare expenses and potential malpractice claims.

Machine learning, deep learning, and statistical analysis have emerged as powerful tools for computer-aided diagnosis, particularly in complex computer vision tasks related to medical imaging,[8,9] such as lung ROI segmentation and diseases classification. Recent developments in deep learning have enabled machines to perform on par with or even surpass humans in various activities, including predicting treatment outcomes like cancer therapy. By leveraging vast labeled datasets and deep learning techniques, significant progress has been made in categorizing thoracic disorders using Computer Tomography (CT), Ultrasound (US), and X-ray imaging[9,10].

Machine learning is a subset of artificial intelligence that involves developing models used for training and decision-making based on extensive datasets. It plays a crucial role in tasks requiring human-like intelligence, such as voice recognition, translation, and image analysis[11]. Deep learning, a subset of machine learning, has shown significant success across various industries, particularly in healthcare. Deep learning models can accurately predict and categorize diseases such as lung cancer, pneumonia, and COVID-19 using medical images, helping humans in the diagnostic process[12].

As deep learning models grow larger and more complex, they acquire deeper data representations, leading to enhanced effectiveness. By employing a combination of non-linear functions, deep learning algorithms yield more accurate outcomes, further advancing the field of medical diagnosis and treatment[13].

In the field of deep learning, the core objective is to extract and classify features from images, a task at which deep learning has excelled across various industries, including healthcare[14]. Deep learning models have demonstrated remarkable capabilities in accurately predicting and diagnosing illnesses using medical images, including pneumonia, lung cancer, and COVID-19, without requiring human expertise. Unlike traditional machine learning approaches, deep learning techniques leverage the growing size of neural networks to automatically capture and analyze data, leading to more precise findings. These models describe features using a series of non-linear functions, optimizing the accuracy of the overall model[15].

In many countries, chest computed tomography (CT) and X-ray images are commonly used for lung diseases detection, as clinical imaging plays a crucial role in identifying the disease. Early diagnosis of diseases like lung cancer is imperative for improving survival rates[16]. Machine learning and image processing techniques have shown significant promise in enhancing the diagnosis of lung cancer. This section provides an extensive evaluation of deep learning models for COVID-19, lung cancer, and pneumonia[17,18].

The application of pre-trained models, such as VGG-16, ResNet-50, and InceptionV3, to clinical images of lung diseases and COVID-19 has yielded promising results[19]. Notably, pneumonia is a major symptom of COVID-19, and pre-trained models have facilitated the identification of pneumonia as a key manifestation of COVID-19. Studies have shown that models trained to detect viral pneumonia can effectively identify COVID-19 as well. Here, the feature extraction process, as discussed in[20], plays a crucial role in identifying relevant patterns from the clinical images. To diagnose COVID-19 pandemic, neural network approach was employed to extract visual features from volumetric chest CT images. The results demonstrated superior performance compared to existing methods[20]. Previous research employed pre-trained models-based convolutional neural network (CNN) architectures, including Inception-ResNetV2, ResNet152, ResNet50, InceptionV3, and ResNet101, to identify COVID-19 pneumonia based on X-ray images[21].

A detailed relation extraction neural network (DRENet) learning-based CT diagnostic algorithm was employed to identify COVID-19 patients, achieving a recall of 0.93, an AUC of 0.99, and an accuracy of 0.96[22]. This research highlighted the potential of deep learning based on CT scans to detect COVID-19 patients and automatically identify abnormal changes. Another study categorized COVID-19 Chest X-ray images using MobileNet and ResNet architecture. This approach dynamically combined characteristics from multiple CNN layers to address the gradient problems and outperformed current methods by 99.3% on the CT images dataset and by 99.6% on the X-ray.

Additionally, several deep learning-based methods for pneumonia classification have been discussed in the existing literature. These include a very deep CNN with 121 layers, localization approaches based on pre-trained DenseNet-121, and novel multi-scale heterogeneous three-dimensional (3D) convolutional neural networks (MSH-CNN) based on chest CT images[23]. Additionally, hierarchical CNN structures like Mask-RCNN, 3D deep CNNs, and combining outputs from different neural networks have also been employed for pulmonary image segmentation and pneumonia identification. While most approaches focused on individual neural networks, Hashmi et al.[24] combined outputs from ResNet50 for the final prediction of pneumonia disease.

The study by Malik H et al[25] introduces a multiclass deep learning classification model for pneumonia detection. The primary objective of the research is to develop a deep learning framework capable of classifying multiple classes, including Pneumonia, Lung Cancer, TB, Lung Opacity, and most recently COVID-19.

In the pre-processing phase presented in[26], X-ray images are applied as inputs, and the final output of the model is the categorization of the input X-ray image at the disease level.[26]

This phase involves initial preprocessing steps such as normalization, resizing, and random splitting of data images into 80% training and 20% validation sets. Subsequently, deep learning algorithms are employed in the feature extraction and classification phases.

In a related study, automated techniques were employed to classify chest X-rays into pneumonia and disease-free classes using nine deep learning architectures[27]. These architectures include CNN, DenseNet201, VGG16, VGG19, Inception, ResNet-V2, Inception-V3, Xception, Resnet50, MobileNet-V2.These models have demonstrated high accuracy but often require extensive computational resources and large datasets. Interestingly, hybrid approaches, such as the combination of CNNs with SVM classifiers, have shown promise in improving classification accuracy while optimizing computational efficiency. Our study builds upon these prior methodologies, leveraging the strengths of VGG16 and SVM to achieve improved performance in lung disease detection.

Experiments were conducted using a dataset consisting of 5856 images from CT scans and X-rays, comprising 1583 normal images and 4273 pneumonia images. The performance of the models was evaluated using various performance metrics. The results indicated that MobileNet-V2, Inception_Resnet-V2, and Resnet50 achieved highly accurate results, surpassing 96%. Moreover, it was suggested that employing larger datasets and more sophisticated feature extraction techniques based on deep learning image segmentation could further enhance performance.

The primary objective of this study is to develop and validate a deep learning-based classification model, integrating VGG16 with an SVM classifier, for the accurate detection of multiple lung diseases, including COVID-19, pneumonia, and lung opacity, using chest X-ray images. This approach aims to enhance diagnostic efficiency, providing a robust and reliable tool for clinical applications.

Materials and Methods

Data description

In this study, the Chest X-ray image dataset was obtained from publicly available sources[28-31] which provided images categorized into four classes: COVID-19, Lung Opacity, Normal, and Viral Pneumonia. The dataset comprised a total of 7811 images, with 5468 images allocated for training and 2343 images for testing, all in JPEG format.

The Chest X-ray images were obtained from multiple publicly available datasets referenced in[28-31], specifically:

- **Rahman et al.**[28] explored COVID-19 detection using enhanced Chest X-ray images from multiple sources, including the COVQU dataset consisting of 18479 normal, non-COVID lung opacity and COVID-19 CXR images.
- **Islam et al.**[29] used a combination of publicly available datasets (radiography-database), which include images categorized into COVID-19, Non-COVID, Viral Pneumonia, and Lung Opacity (The database includes 3616 COVID-19

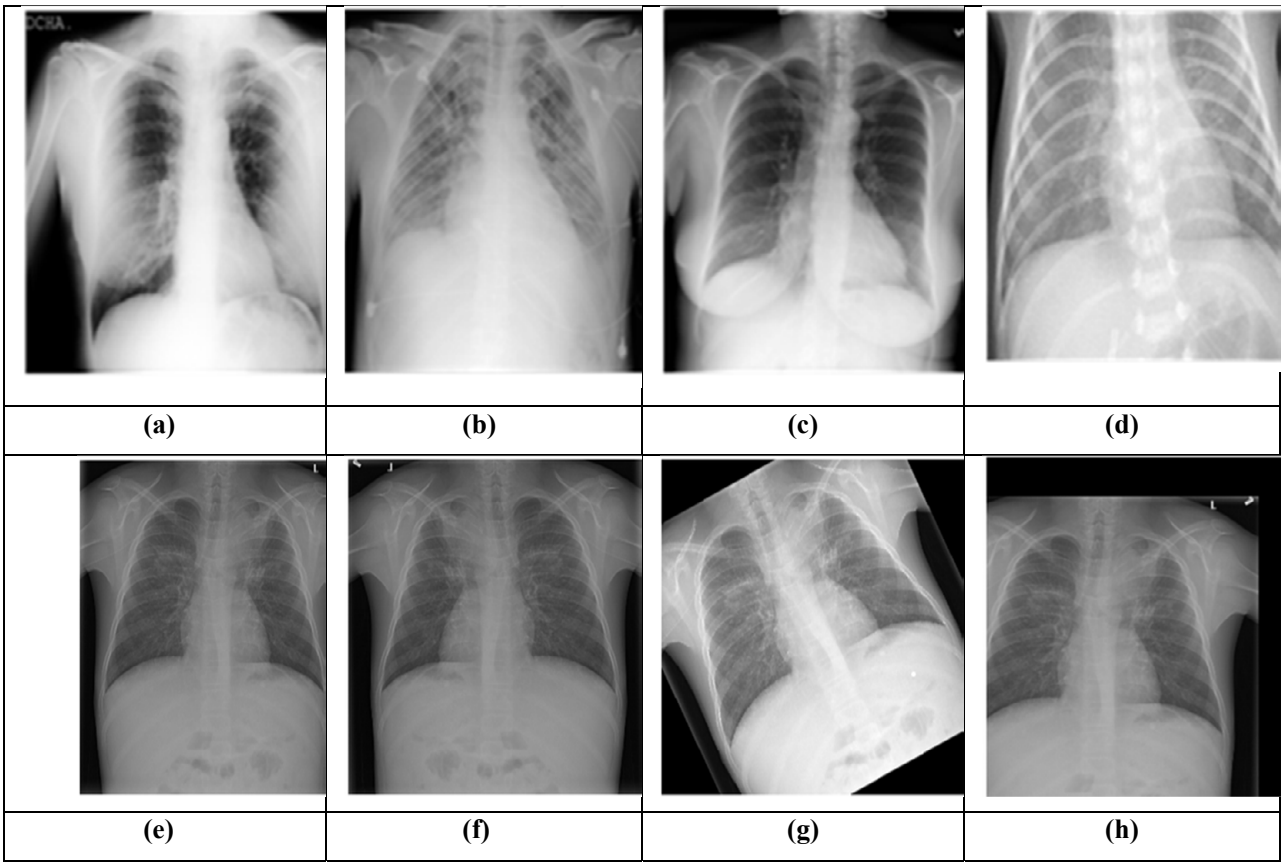


Figure 1. Exemplary X-ray images displaying the COVID-19, Lung Opacity, Normal and Viral Pneumonia categories, and data augmentation.(e) Image original, (f) Horizontal Flip, (g)Rotation, (h) Translation.

cases along with 10192 normal circumstances, 6012 Lung Opacity (Non-COVID lung infection), and 1345 non-COVID viral pneumonia images).

- **Muljo et al.**[30] utilized two datasets COVID-19 radiography database and the National Institutes of Health (NIH) Chest X-ray, the first dataset contains COVID-19, Normal, Pneumonia and lung opacity (3616 COVID-19 positive cases are represented along with 10192 normal, 6012 lung opacities (non-COVID), as well as 1345 cases of viral pneumonia) and a second dataset containing 112000 chest X-ray images are available through NIH Chest X-rays.
- **Tsai et al.**[31] presented the RSNA International COVID-19 Open Radiology Database (RICORD), which includes annotated Chest X-ray images focusing on COVID-19 diagnosis.

Figure 1 illustrates representative images from the four X-ray classes (see first row of **Figure 1**). Each image in the dataset had 256 grey levels and dimensions in pixels. Additionally, device and computer specifications included resolutions in inches and pixels.

The Data augmentation was performed on the training set to further enhance model robustness. We applied random rotations (the rotation factor is 0.2 (rotation between -72° and +72°)), horizontal shifts, and translation (±20%). These augmentations increased the diversity of the training data, improving the model's ability to generalize data (see second row of **Figure 1**).

The research methodology involved several stages, including data collection, processing of X-ray images related to COVID-19, Lung Opacity, normal cases and Viral Pneumonia, selection of a pre-trained network for transfer learning, categorization of X-ray images using CNN-based transfer learning, assessment of performance across various CNN-based transfer learning techniques, and comparison of performance against other methods for classifying X-ray images associated with COVID-19, Lung Opacity, Normal, and Viral Pneumonia[28-32].

Convolutional Neural Network

Medical image classification has widely adopted Convolutional Neural Networks (CNNs) because their architecture is specifically designed to automate feature extraction, reducing the need for manual intervention[33]. The CNN framework was effectively used for the classification of various lung disease types. Lung classification can be accomplished either by applying CNN on small patches or by employing Fully Convolutional Networks (FCNs) on the entire image. As illustrated in **Figure 2**, the proposed CNN architecture consists of 2 convolutional layers, succeeded by a 2 × 2 Max Pooling layer, and lastly, a flatten layer and a fully connected (FC) layers[34,35].

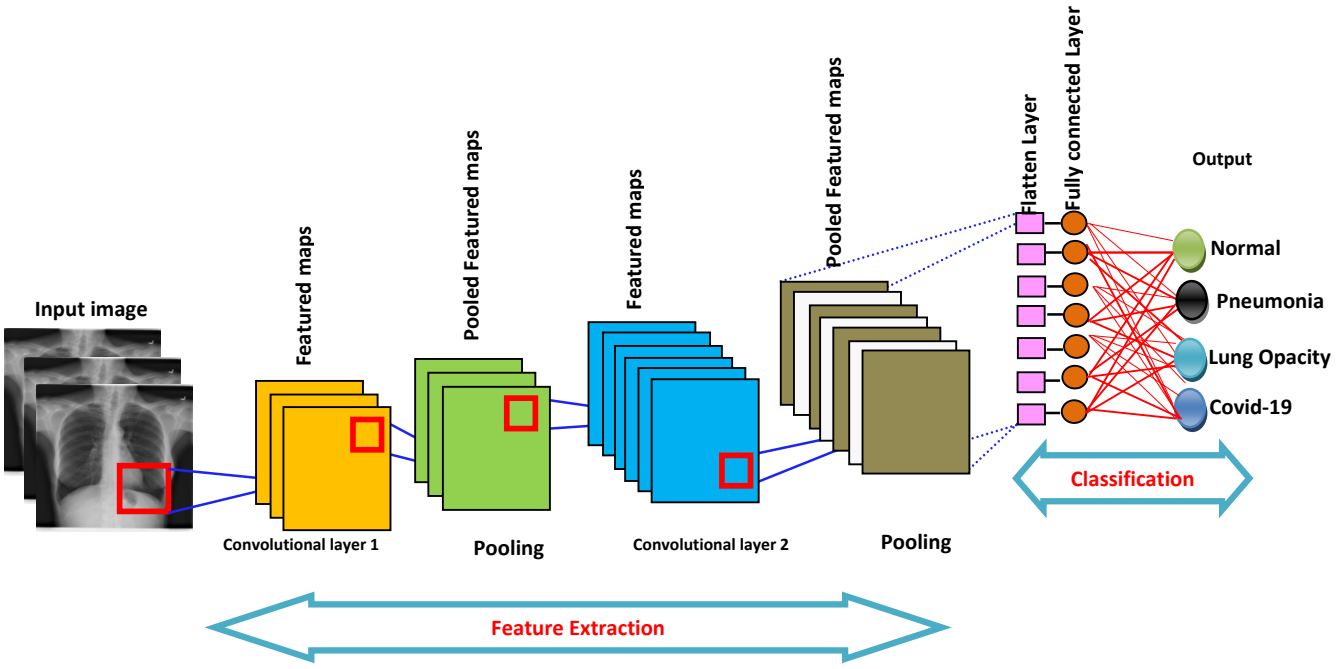


Figure 2. CNN architecture in lung diseases classification based on X-ray images.

Preprocessing stage

Due to the distortion introduced by the inclination field in Chest X-ray images, an initial pre-processing step is first carried out. In order to rectify the bias field distortion in the X-ray sequences, the filtering method[36] is employed for each image. Prior to training, all images were resized to 224x224x3 pixels, to match the image size with the network input. The intensity normalization was applied to standardize the pixel values across images. This ensures that the characteristics of each class are preserved.

The data distribution for the proposed VGG16-SVM model is depicted in **Figure 3**.

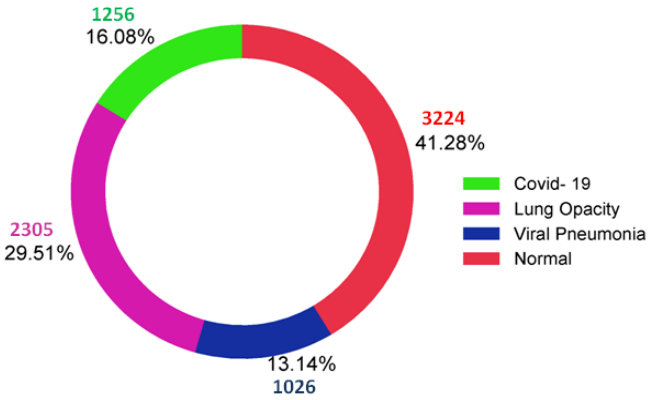


Figure 3. Data distribution displayed in different classes (COVID-19, Lung Opacity, Viral Pneumonia, and Normal).

Training and test process

There is no standard or commonly used dataset available for the training and testing processes involved in lung disease classification, which poses challenges for consistent model evaluation and benchmarking. Therefore, we applied a cross-validation approach for the proposed VGG16-SVM model in the X-ray datasets, along with the manually annotated ground truth lung masks. Each set contains 30% of the X-ray data, selected randomly for validation purposes from the entire dataset[37]. The validation set is used during model tuning.It helps in adjusting the model and preventing overfitting, while the test set is reserved for evaluating the final performance of the model, ensuring an unbiased assessment.

Indeed, the training set is the most essential dataset. We conducted training and testing of the classification technique a total of five iterations. Afterwards, the average of the accuracy values derived from the test datasets using the trained classification model was computed.

Classification model in lung diseases

As depicted in **Figure 4**, the grading method utilizes VGG-16, where a classifier is pre-trained using a convolutional system centered on the VGG-16 network[38]. The convolutional weights for the VGG-16 network can be acquired from the source[36].

The convolutional base comprises five series of convolutional layers with ReLU activation functions, each subsequently followed by a max-pooling layer. The proposed classification method includes a flatten layer to convert the data from 3D to 1D, a Dropout layer to alleviate overfitting, and ultimately a densely connected layer with the Sigmoid activation function serving as the output layer. The input and output layers possess dimensions of 256 × 256 × 3 and 1, respectively. The grading model was constructed using Keras-TensorFlow[39]. The used datasets have been divided into four categories.

Data augmentation is used on the training X-ray images through random operations such as rotations and translations. Extra training samples were generated in each training epoch. Multiple instances were generated to ensure effective training of the network over 30 epochs.

In the validation process, linear transformations are applied to avoid the identification of non-real lung structures. The parameters employed in image augmentation are detailed in Table 1. The images resulting from different augmentation techniques are illustrated in **Figure 4**. Only one of these techniques was employed to produce each augmented image.

An overview of the implementation methods

The expected abnormal lung masks were generated from the X-ray images using the VGG16-SVM classification model. These masks were then utilized to identify representative images for three categories of lung diseases (COVID-19, Lung Opacity, and Viral Pneumonia) from among the normal X-ray images[40]. Patients were selected so that the cross-sectional lung areas affected by the disease, as estimated from the respective predicted masks, comprised approximately 50% of the largest region of interest cross-sectional area within the entire X-ray image for each patient. This criterion helps to eliminate false positive lesion predictions from the classification model, ensuring that the selected images contain pertinent information about lung diseases, including details regarding area size and irregularities in the shape of infected lesions.

The project used the COVID-19 radiography database as its dataset, which comprises a total of 21165 Chest X-rays (CXRs) across 4 distinct classes (COVID-19, Lung Opacity, Normal, and Viral Pneumonia)[41].

The data importance is primarily centered on the abnormal lesion and gradually reduces towards the irregular edges.

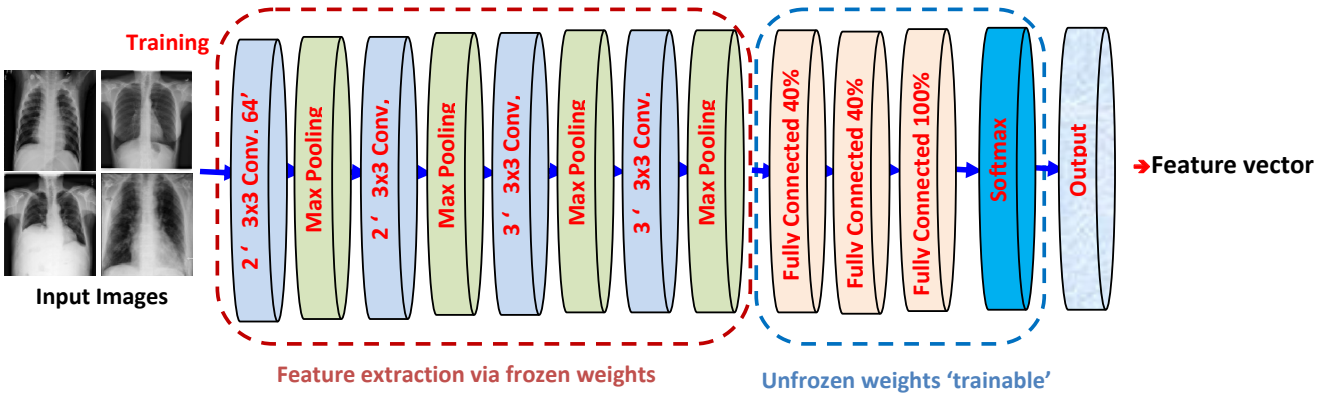


Figure 4. The proposed methodology using VGG-16 for X-ray classification.

From the selected X-ray images of diseases and normal cases (755 in total), each sized (256 × 256 × 3), testing and training datasets were created and used for training and validating the classification method. The optimizer technique was Adam, with a learning rate set to 5×10^{-5} for the training process. This value was selected based on hyperparameters tuning, where different rates were tested, and it provided the best stability and convergence during the model training.

The training process covered 30 epochs with a batch size of 10. Uniform data augmentation,[42] including shift, zoom, and shear operations with a range of 40%, was applied to mitigate overfitting risks with a limited X-ray dataset. Following training, the grading model was employed to predict the classes of lung diseases for the selected X-ray images of each analyzed patient.

MobileNetV2 deep learning model

MobileNetV2 is a convolutional neural network (CNN) design specifically optimized for efficient performance on mobile platforms[43]. Its architecture diverges from conventional CNN designs by establishing connections specifically between bottleneck layers.

Moreover, the intermediate expansion layer employs profound convolutions to extract nonlinear features effectively. The MobileNetV2 structure comprises an initial convolutional layer stack of 32 layers, succeeded by 19 bottleneck layers. The specifics of the MobileNetV2 model's design are depicted in **Figure 5**. In this research, we introduce a MobileNetV2 configuration employing two innovative fine-tuning methodologies to classify different X-ray images (see **Figure 5**).

Res-Net50 for lung diseases classification

In this research, we adopted the Res-Net-50 model to demonstrate its flexibility in classifying complex lung ROI[44]. The subsequent application of the classification method effectively categorizes lung disease types in X-ray images using the Res-Net approach.

Therefore, we propose the adoption of the Res-Net approach for lung disease classification in X-ray images, as depicted in **Figure 6**. Given that the CNN method allows for the application of all information within the input data, including features identified in convolutional networks, feature extraction and optimization procedures are conducted through the convolutional architecture. Within the classification system of three lung diseases compared to normal cases, the primary X-ray images analysis is on the training process, which constitutes 70% of the entire database, while the validation and testing processes collectively account for the remaining 30%.

- **Res-Net structure**

Within the Res-Net framework, various Res-Net variations with 18, 34, 50, 101, and 152 layers have been developed. Each layer of the Res-Net model is divided into numerous blocks, namely the identity block (Ib) and the convolutional block (Cb), which constitute the Res-Net methodology. In this work, we employed Res-Net-50 for X-ray image classification[45].

We opted for Res-Net-50 in this investigation due to its deeper architecture compared to Res-Net-34 and notably fewer parameters compared to Res-Nets 101 and 152, resulting in expedited training times. The used Res-Net-50 architecture is depicted in **Figure 7**.

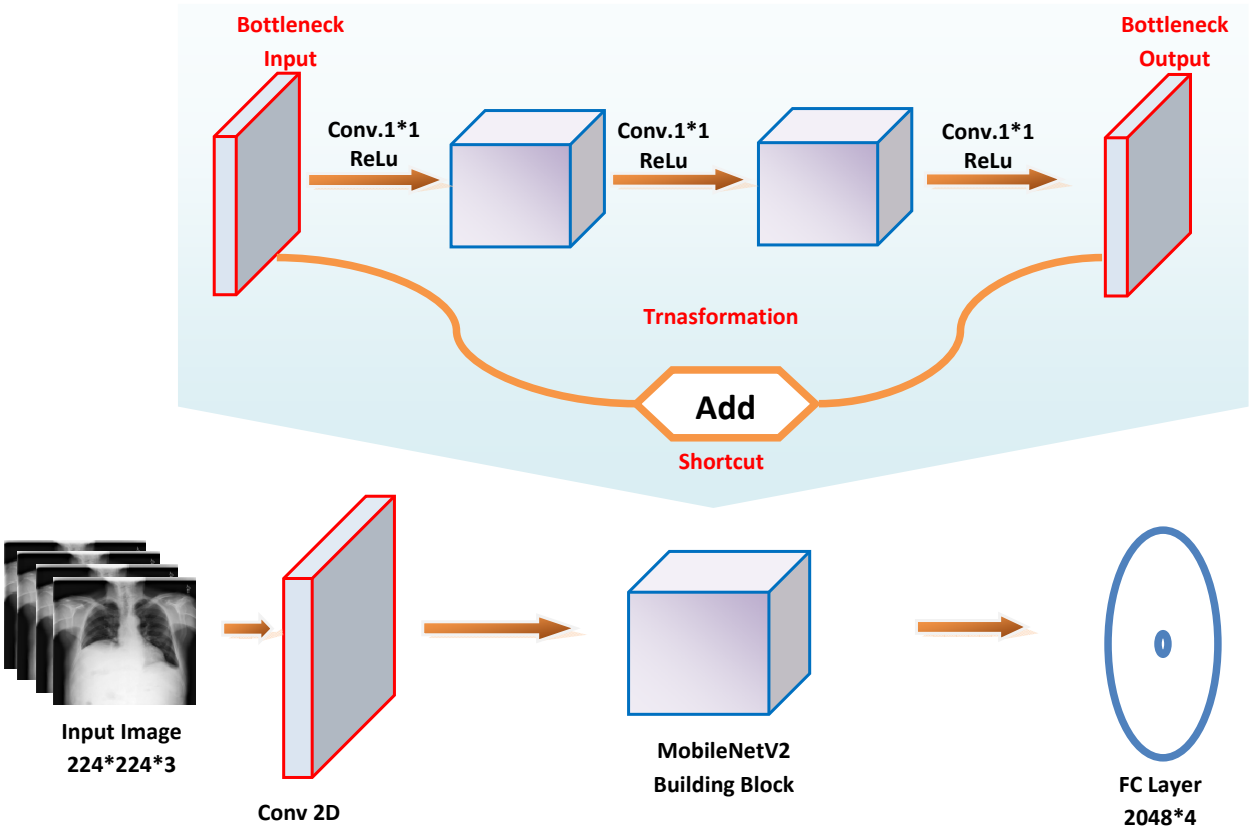


Figure 5.TheMobileNet V2 learning architecture.

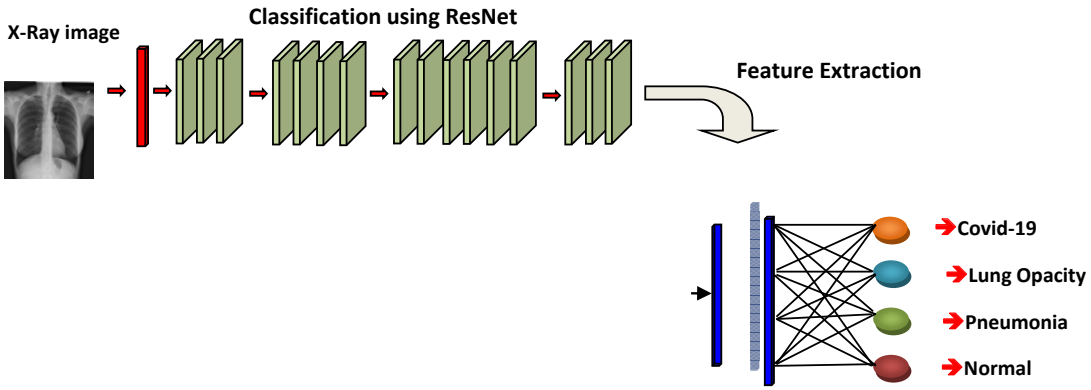


Figure 6. Lung disease classification based Res-Net structure.

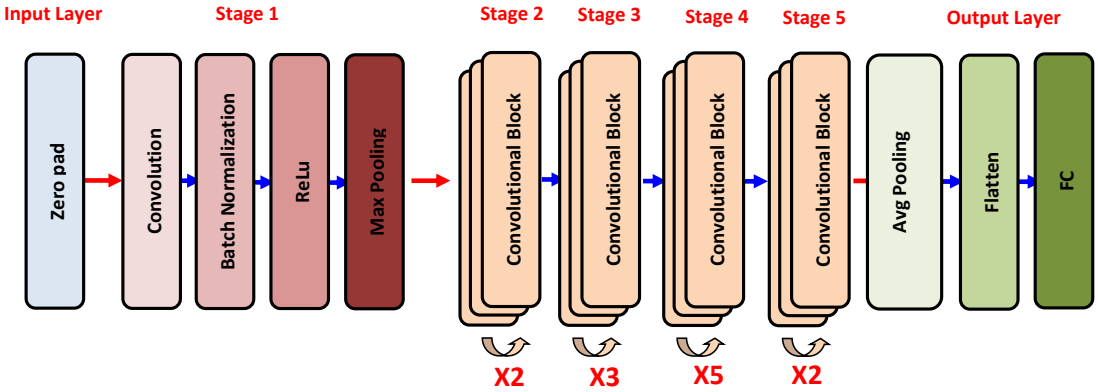


Figure 7. Res-Net architecture.

The model's input underwent initial processing with zero-padding using 'Zero Pad' (3,3) and comprised five stages, each consisting of a convolution block and an identity block. In the output layer, 2 × 2 Average Pooling ('Avg Pooling') was applied, followed by flattening the output. A fully connected (Dense) layer was employed to condense the input to the number of classes, using the softmax activation function.

The output of each residual layer is connected to its own input, which then serves as the input for the subsequent layer. The network operates without any fully connected layers, aligning with the valid section of each convolution.

The function K(x) introduces the residual mapping to form a residual learning block, with only two layers stacked. The equation "K(x) = F(x) + x" is approximately computed by the Res-Net block after identification by the feed forward neural schemes via shortcut networks. A shortcut establishes a connection between distant layers without requiring the full set of layers. These shortcut connections combine the output of stacked layers with the input through an identity mapping process without introducing additional parameters. This aids in the flow of gradients, leading to faster training, particularly with the addition of more layers.A recent enhancement to Res-Net involves introducing additional identity connections within the network. This approach promptly facilitates gradient backpropagation to earlier layers, simplifying the training process.

• Identity Block

The identity block is characterized as follows:

$$y = F(x, \{Wi\}) + x \quad (1)$$

"x" and "y" represent both of input and output layer vectors. The trained residual mapping is denoted as "F(x, {Wi})."

The identity block preserves equivalent dimensions for both "x" and "F." The lower and upper paths depict the primary routes and the shortcut, respectively. Channel-wise normalization is attained through Rectified Linear Unit (ReLU) and Batch Normalization (BN) functions, serving as nonlinear activation functions. Ultimately, the shortcut and the input are combined before applying the ReLU activation function.

• Convolutional Block

In the convolutional block, there is a difference between the input and output dimensions [41]. The shortcut networks accomplish a linear projection denoted as "Ws," which is used to adjust the dimensions between "x" and "F.

$$y = F(x, \{Wi\} + Wsx) + x \quad (2)$$

"x" represents the input, while "y" denotes the combined output vector of the convolutional block. "F" indicates the output of the stacked layers. The differentiation between the identity block and the convolutional block is underscored in the shortcut pathway by incorporating a 2D convolutional layer. A filter size of (1 × 1) and a stride of (*s*, *s*) have been utilized by the 2D convolutional layer to align with the output dimensions. The input is resized to match the dimensions of the primary path in this shortcut. The enhanced shortcut is integrated into the main path output. The primary enhancement of the improved shortcut lies in its ability to address the vanishing gradient problem, as illustrated in **Figure 8**.

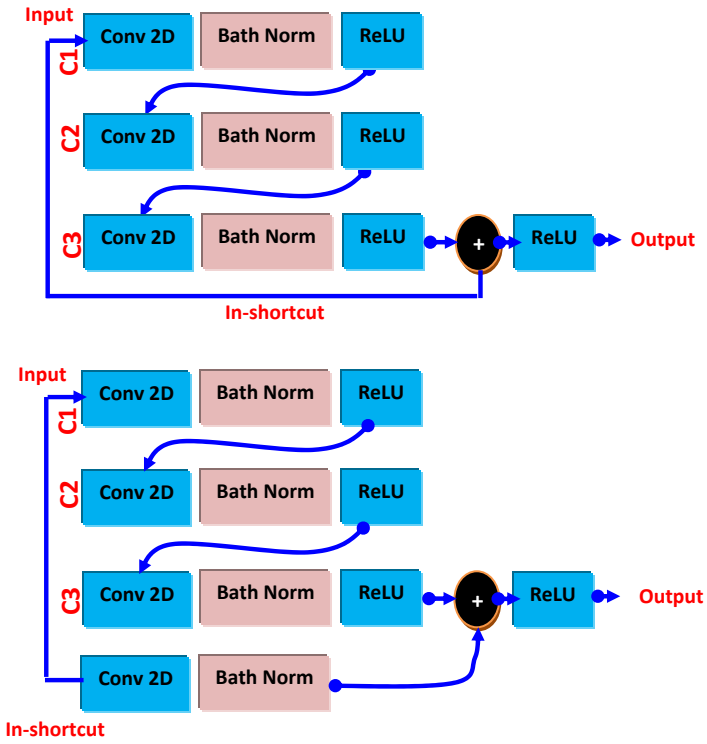


Figure 8. The identify and convolutional blocks
***component 1 (C1), component 2 (C2), component 3 (C3).**

Inception-V3 CNN architecture for lung abnormalities classification

The Inception-v3 architecture strives to reduce the resource consumption of Deep Convolutional Neural Networks (DCNN), which shares common features with Network in Network models[46]. Illustrated in **Figure 9**, the Inception model relies on employing the following key components to capture the variability of the dataset while justifying general source procedure.

Xception CNN architecture for lung diseases classification

The Xception model was introduced by Francois Chollet[47]. Xception ranges the Inception architecture by replacing the standard Inception modules with modified depthwise separable convolutions, which enhances its performance on both the ImageNet ILSVRC and JFT datasets.

The modified depthwise separable convolution consists of a pointwise convolution followed by a depthwise convolution. Additionally, residual/skip connections, as proposed in the ResNet architecture, are incorporated[48].

The Xception architecture comprises three blocks: entry flow, middle flow, and exit flow. The middle flow block is repeated eight times. Notably, there is no intermediate non-linearity in the modified depthwise separable convolution within the architecture. The pre-trained model of Xception used in the paper is depicted in **Figure 10**.

In the area of medical imaging, the Inception architecture is commonly utilized for categorizing anomalies, particularly in assessing disease progression, such as in instances of lung cancer[49], kidney cancer[50].

By integrating various filters of diverse dimensions at the same network level, it becomes possible to capture information across a range of scales.

However, this approach entails an increase in resource consumption as it involves computing more parameters compared to using only a single filter. To mitigate the resource consump-

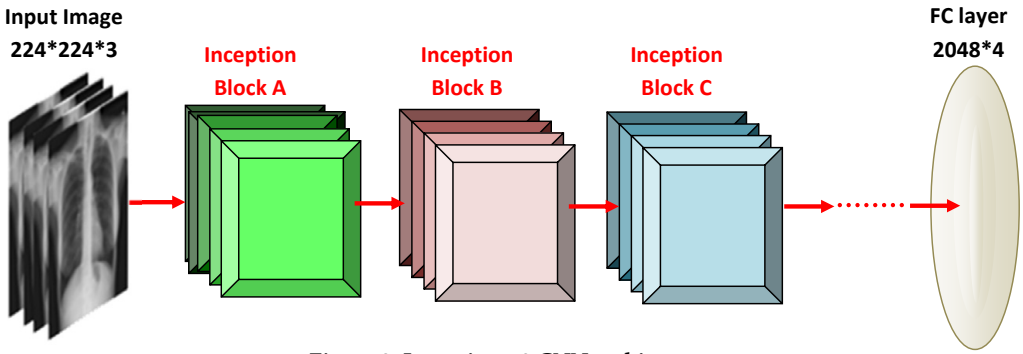


Figure 9. Inception-v3 CNN architecture.

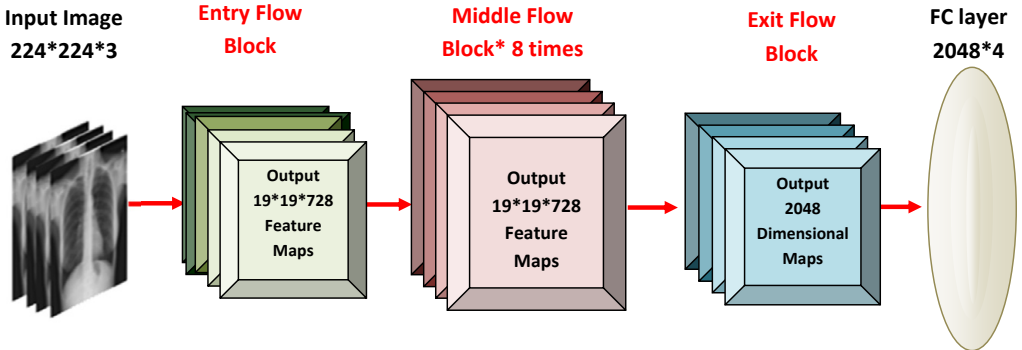


Figure 10. Xception CNN architecture.

tion associated with employing multiple filters, a mathematical technique is employed to reduce the image dimensions processed by the 3x3 and 5x5 filters. This is accomplished by introducing a preliminary 1x1 filtering step.

The 1x1 convolution size performs a pooling operation on pixel values within the image's spatial dimensions. For example, after applying the 1x1 convolution, if the input image consists of 3 channels (RGB), the output image will be reduced to 1 channel.

Dimension reduction enables the preservation of information while simultaneously reducing resource expenditure during the subsequent convolution phase employing a 3x3 filter.

The Dense-Net Architecture in classification process

The DenseNet architecture is efficiently used for COVID-19 classification task, DenseNet variants[51] are in line with deep CNNs (DCNNs). Each network layer receives the outputs from the preceding layers as its input. Illustrated in **Figure 11**, this characteristic augments the total number of network connections in a conventional configuration of L CNN layers, where each layer is connected to every other, to [L(L-1)]/2.

The network is partitioned into dense blocks, wherein the dimensions of the feature maps remain constant within a block while the number of filters varies between them. DenseNet offers numerous benefits, including a substantial reduction in the number of parameters, the reprocess of features, and the justification of the gradient problem.

Although the DenseNet architecture adopts a similar approach to the ResNet architecture by integrating short connections between layers, it differs significantly in its manner of incorporating information from previous layers. Let's contemplate a network comprising L layers, where each layer applies a non-linear transformation denoted as Hl(·), with 'l' representing the layer index. The output of the l^{th} layer is denoted as X_l. If the network follows a ResNet architecture.

$$X_l = H_l(X_{l-1}) + X_{l-1} \tag{3}$$

If the network follows a DenseNet architecture, then

$$X_l = H_l\left(\left[X_0, X_1, ..., X_{l-1}\right]\right) \tag{4}$$

In the DenseNet architecture, the concatenation of information leads to a reduction in the number of parameters by a factor of 3 compared to the ResNet architecture. This reduction is accomplished while preserving the same level of performance in terms of accuracy.

The proposed lung diseases classification using VGG-16+SVM model

The classification process using VGG-16+SVM approach involves categorizing subjects into three groups based on various lung diseases: Viral Pneumonia, COVID-19, and Lung Opacity, compared to normal cases[52]. Using the SVM classifier, the classification procedure is divided into two phases: the training phase and the validation phase. During the training phase, the majority of the database (70%) is used to train the network, while during the validation phase, the smaller portion of the X-Ray image database (30%) is used by the SVM technique.

The dataset is split into two categories: 5468 training samples and 2343 validation cases. This asymmetry in the dataset split ensures a significant learning process for the network and aims to achieve improved classification results. Throughout the training process, the structure of VGG16 is developed to ensure the feature extraction process. The network comprises an input layer with a reduced number of features (2 features after processing by the VGG-16 model), a single hidden layer with 30 neurons, and an output vector.

After feature extraction stage using VGG16, the input features of the SVM method is used to classify X-ray images into 4 classes.

The target outputs for each case are predefined as follows: '-0.9, 0.9, 0.9, 0.9' for the COVID-19 case, '0.9, -0.9, 0.9, 0.9' for the Lung Opacity case, '0.9, 0.9, -0.9, 0.9' for the Pneumonia case, and '0.9, 0.9, 0.9, -0.9' for the normal case. The optimal number of neurons in the hidden layer is determined through a series of experiments to achieve the lowest error rate and the highest classification accuracy. The optimal structure of the SVM model is selected based on the hidden layer size that results in the lowest validation error.

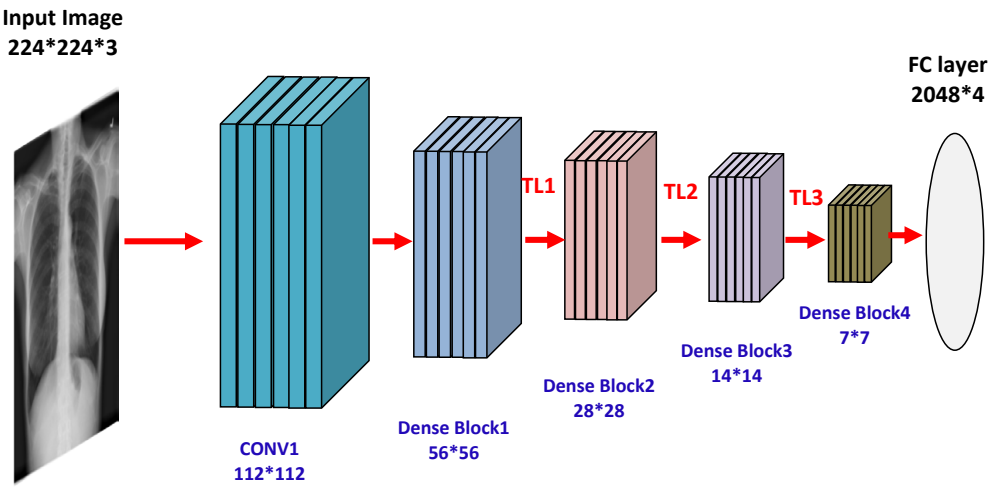


Figure 11. Dense-Net model.

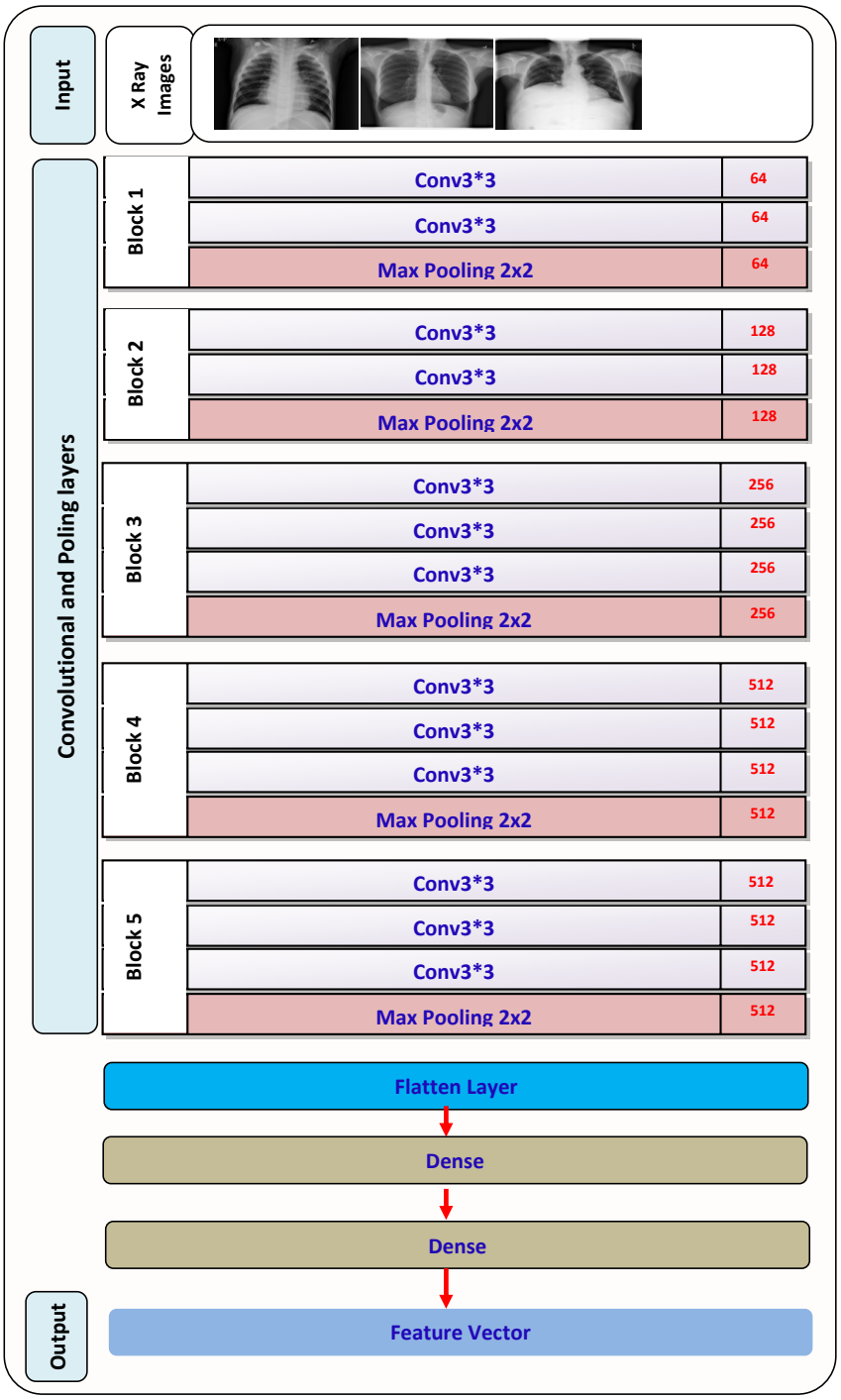


Figure 12. The proposed VGG-16 architecture.

• Convolutional Blocks and Pooling Layers in VGG-16

In the VGG-16 structure, there are five convolutional blocks labeled as Conv-1 to Conv-5. The composition of specific layers within each convolutional block can vary depending on the architecture. However, one or more 2D convolutional layers (also known as pooling layers) are typically included in each convolutional block. Although additional layers may sometimes be present, we will focus on these two types of layers for simplicity.

The architecture consists of multiple convolutional layers with a kernel size of (3x3) followed by max-pooling layers. After the convolutional and pooling layers, a flatten Layer and two dense layers. The final output represents the feature extraction vector, capturing the essential features from the input X-ray image for classification stage (see **Figure 12**).

Combined VGG16-SVM for Multi Lung Diseases Classification

In the present study, we utilized the combined VGG16-SVM model to demonstrate its effectiveness in classifying lung diseases. Here, we employed a classification strategy based on the support vector machine (SVM) method to accurately identify different lung diseases depicted in X-ray images. We propose a combined approach, referred to as VGG16-SVM methodology, for the detection of three lung diseases, as illustrated in **Figure 13**. Following feature extraction, the X-ray images classification phase employs supervised machine learning techniques, particularly the SVM algorithm, to classify the feature vectors into different classes.

In support vector machine (SVM) classification, handling class imbalance where the majority class (more frequent) dominates the

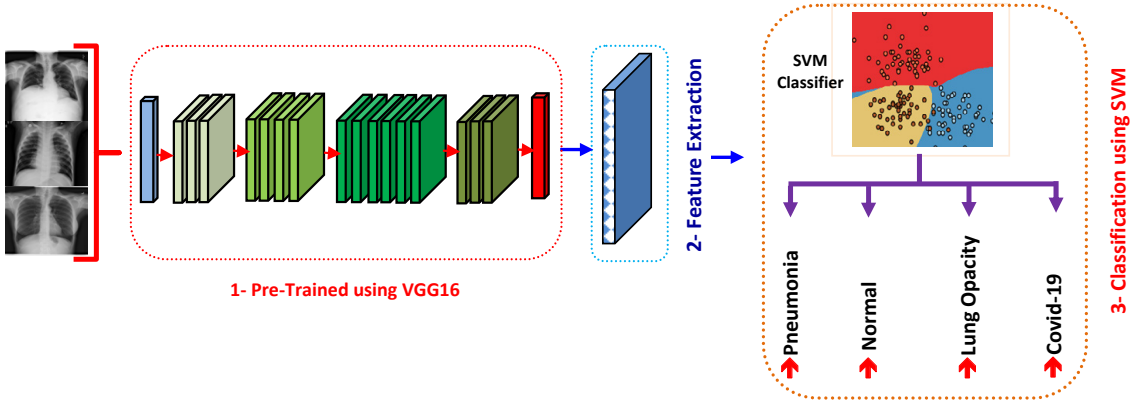


Figure 13. The proposed methodology using combined VGG16-SVM

minority class (less frequent) is crucial to avoid biased predictions. When dealing with imbalanced datasets, the model can become biased toward the majority class, resulting in poor performance on the minority class.

The Class Weights (Weighted SVM) approach is applied to assign higher weights to the minority class and lower weights to the majority class. This can be done by modifying the SVM's loss function that misclassifying instances from the minority class compared to majority class.

The use of convolutional neural network (CNN) approaches, such as VGG-16, enables the application of all available information within the input data for feature extraction and optimization. This allows for the automatic computation of feature sets using convolutional architecture, leading to more accurate and efficient lung diseases discrimination from X-ray images (see **Figure**13).

The proposed methodology is applied VGG-16 and SVM.

Step 1: Pre-trained VGG-16 model is used for feature extraction from the input X-ray images.

Step 2: The extracted features are passed through the network, forming a feature vector.

Step 3: The feature vector is then classified using a support vector machine (SVM) into four classes.

After the flatten layer, we used two dense layers to reduce the number of features. The redundant information has been filtered out to learn pertinent parameters. Thus, the SVM model comprises an input layer from the VGG16 model with a 1D vector contains 512 features, a single hidden layer with 30 neurons, and 4 output neurons with softmax activation function for multi-class classification.

The optimal number of neurons in the hidden layer is determined through a series of experiments to achieve the lowest error rate and the highest classification accuracy

VGG16-SVMPerformance Evaluation

Evaluation metrics play a crucial role in assessing the performance of lung disease classification models in various medical imaging applications. These metrics are commonly used to evaluate the effectiveness of the classification model in distinguishing between different lung disease classes, including COVID-19, Lung Opacity, Viral Pneumonia, and normal cases.

Four evaluation metrics commonly used in this context are accuracy (AC), precision (PR), recall, and F1-score (F1). These metrics are calculated based on the number of true positives (TP), false positives (FP), false negatives (FN), and true negatives (TN) predicted by the classification model.

These evaluation metrics provide valuable insights into the performance of lung disease classification models, helping researchers and clinicians assess the reliability and effectiveness of the models in clinical practice.

$$AC = \frac{(TP + TN)}{(TP + FN + TN + FP)} \tag{5}$$

$$PR = \frac{TP}{(TP + FP)} \tag{6}$$

$$recall = \frac{TP}{(TP + FN)} \tag{7}$$

$$F1 = \frac{2 \times precision \times recall}{precision + recall} \tag{8}$$

Results

The experiments in this study were conducted using Python (version 2.16) as the programming language. Deep learning models were developed and trained using TensorFlow (version 2.16) and Keras (version 2.16) frameworks. Various libraries, including NumPy, Pandas, OpenCV, Matplotlib, Seaborn were used for different tasks such as data manipulation and image processing, and evaluation. The experiments were executed on a laptop with an Intel Core i7-1355U processor (up to 5.0 GHz, 12 MB cache memory), 16 GB of RAM, and an NVIDIA GeForce MX550 GPU with 2 GB of memory. The system was running on windows 10 as the operating system. The total training time for the complete experiment, including both feature extraction and SVM training, was approximately 1 hour and 16 minutes.

Figure 14 presents the original image of the lung diseases containing all the classes obtained after classification process.

The proposed VGG16-SVM based approach for identifying lung diseases using X-ray images has been evaluated using various metrics, including accuracy, sensitivity, specificity, and precision. The assessment involved four classes: COVID-19, Lung Opacity, Viral Pneumonia, and normal cases. The proposed method was compared to other computer-aided methods such as ResNet50[44], DenseNet[51], and Inception-V3[46], MobileNet-V2[43], Xception[47]. The evaluation metrics were computed for each patient in the dataset, and the average values across all patients were calculated.

According to the results presented in **Figure 15**, the proposed VGG16-SVM based method achieved an accuracy average of 93.50%, compared to different CNN algorithms, across the entire X-ray dataset. The p-value, calculated using a Student's t-test, was found to be equal to2.4×10^{-6}, indicating a statistically significant difference in performance between the different used methods. These results suggest that the proposed VGG16-SVM classification technique can reliably assist Pulmonologists by providing a second analysis strategy for unknown cases requiring additional attention.

Additionally, **Figure 15** illustrates the training and validation processes for the proposed VGG16-SVM model over 30 epochs. The **Figure** demonstrates a linear reduction in training error and a simultaneous rise in training accuracy after each epoch. Notably, the model exhibits the smallest training error, indicating a rapid decrease in error rate during training. This further emphasizes the effectiveness of the proposed VGG16-SVM based approach in accurately classifying lung diseases from X-ray images.

The proposed VGG-16-SVM model employed 7811X-rayimages for the classification model, employing a 20-fold

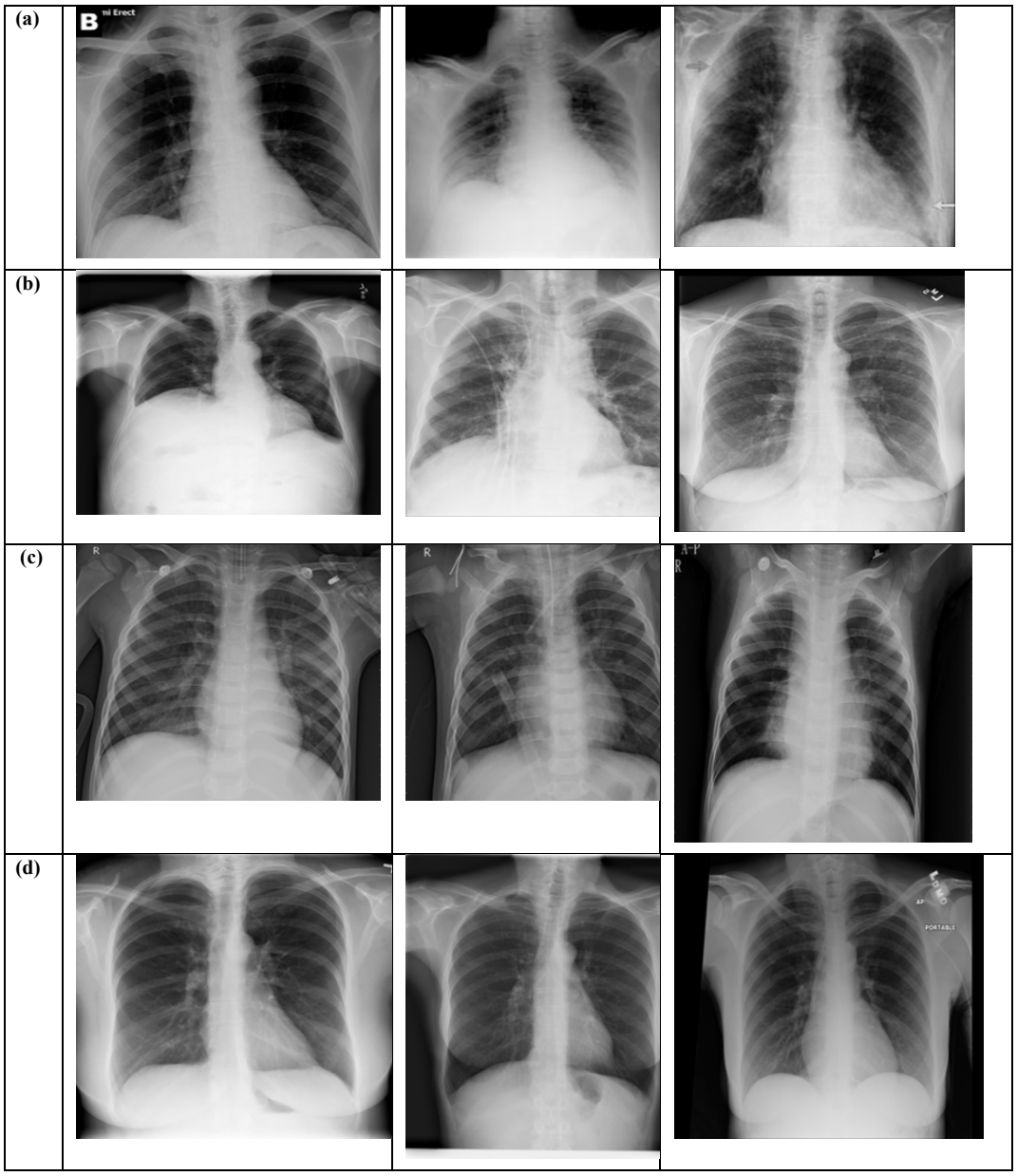


Figure 14. Illustrations of X-ray images classes respectively ((a) COVID-19, (b) Lung Opacity, (c) Viral Pneumonia and (d) Normal).

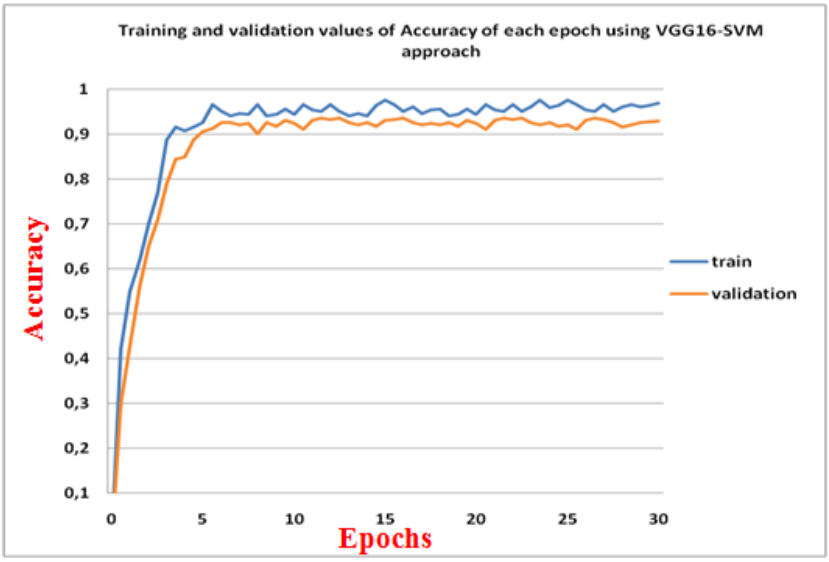


Figure 15. Performance of the proposed VGG16-SVM via (a) Training and validation Accuracy.

cross-validation method, with 14 folds allocated for training and 6 for testing. The selection of 1 out of 20 cross-validation sets is considered a compromise between the quantity of train-validation datasets and the size of the training data necessary for estimating model accuracy.

At the X-ray image level, the proposed classification model present efficient accuracy precision and sensitivity values. The models presented raise specific concerns that could be attempted in future improvements. The main aim is to improve the generalizability of the models, especially the discrimination model, considering the relatively restricted number of images available. Hence, it would be beneficial to explore and contrast the outcomes of these network methodologies with the suggested framework. Moreover, the suggested transfer

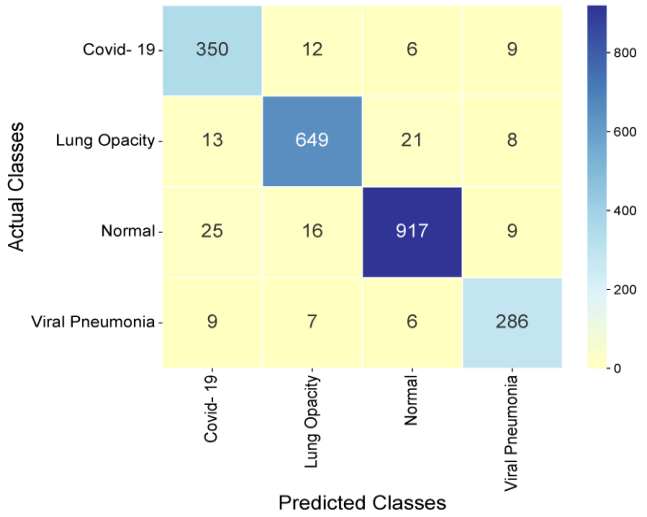


Figure 16. Confusion matrix for the prediction models presenting the precision of the true and predicted lung diseases from X-ray images dataset.

learning employed a relatively simple network architecture utilizing a hybrid design, which is considered appropriate for the dataset utilized in the present study for training and validation. It will be our future study to expand this approach not only to categorize X-ray images into 4 groups but also to identify the disease's characteristics within the images.

A confusion matrix is employed to encapsulate the diagnostic accuracy of the utilized VGG16-SVM model (refer to **Figure 16**). The categorization of distinct lung diseases is conducted using VGG16-SVM. These findings are appropriate with the lung disease categories compared to classification models using ResNet50[44], DenseNet[51], Inception-V3[46], MobileNet-V2[43], and Xception (see **Figure 17**)[47].

The precision measure involves accurately identifying patients with specific lung conditions within the overall population affected by the same disease[52]. In medical imaging, precision often holds greater significance than accuracy, as it is crucial to detect and assess patients showing signs of progress in lung disease severity. Consequently, metrics such as Precision, F1-score, and recall are particularly relevant for providing a comprehensive quantitative analysis of the proposed method in comparison with different techniques reported in the literature (see **Figure 17**). Unlike studies focusing completely on end-to-end CNNs, this study integrates an SVM classifier, which leverages the discriminative features learned by VGG16, improving performance in multi-class classification tasks.

Discussion

Data preprocessing played a crucial role in improving model accuracy and generalizability. Standardizing image dimensions and applying intensity normalization helped reduce variability among X-ray images. The use of 20-fold cross-validation provided a robust evaluation of model performance, ensuring that the results were not biased toward specific data subsets. These preprocessing steps, combined with careful model tun-

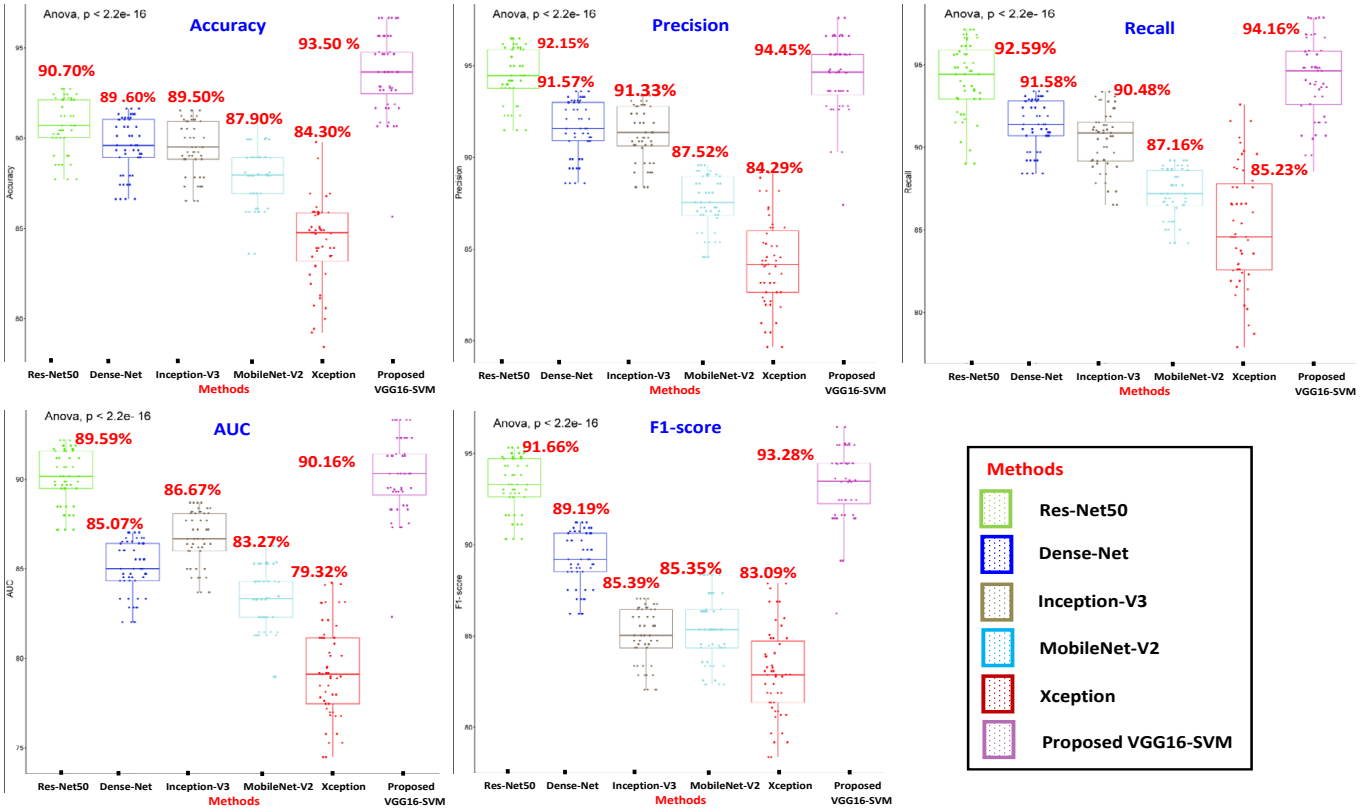


Figure17. Box plots of the accuracy, AUC, recall, precision, and F1-score distribution for the X-ray datasets used for validation of classification model using Xception, MobileNet-V2, Inception-V3, Dense-Net , ResNet50 and the proposed VGG16-SVM. The red percentage labels denote the average values across all datasets for each metric.

ing, contributed to the high precision, recall, and F1-score observed in our study.

The results of this study demonstrate the effectiveness of the proposed VGG16-SVM model for lung disease classification using chest X-ray images. Compared to existing deep learning models such as ResNet50[44], DenseNet[51], Inception-V3[46], MobileNet-V2[43], and Xception[47] (see **Figure 17**), our approach achieves superior accuracy while maintaining computational efficiency. The combination of a pre-trained VGG16 feature extractor with an SVM classifier allows for improved generalization and robustness, addressing some of the limitations observed in purely CNN-based models. This hybrid approach effectively enhances feature extraction, enabling better discrimination between COVID-19, pneumonia, lung opacity, and normal cases.

When comparing our results to previous studies, our model achieves a classification accuracy of 93.50%, which is higher than that of traditional deep learning-based approaches. For instance, Hashmi et al.[24] employed a DenseNet-121 model and achieved 91.60% accuracy, but their study faced challenges related to overfitting due to the lack of an optimized classification strategy. Similarly, Malik et al.[25] developed a multi-class deep learning framework, but their model struggled with class imbalances, leading to lower recall for less-represented categories. By integrating an SVM classifier, our model successfully addresses this issue by applying class-weighted optimization, ensuring better classification performance across all categories.

Indeed, existing models[53-56] such as CNN architectures have reported high recall level but often lack robustness across all performance metrics, such as F1-score and AUC.

Compared to these, the VGG16-SVM model provides a balanced trade-off between precision and recall, essential for minimizing both false positives and false negatives in clinical applications. Prospective studies involving real-time clinical environments are needed to evaluate the model's practical utility and performance in diverse settings.

However, some limitations must be considered. The dataset used, while extensive, may not fully capture the variability seen in real-world clinical scenarios. Although data augmentation techniques such as random rotations and translations were applied to mitigate class imbalances, the model's performance could benefit from additional training on a more diverse dataset[55,56]. Furthermore, the exclusive use of chest X-ray images presents constraints, as combining other imaging modalities, such as CT scans, could provide more comprehensive diagnostic insights.

Despite these advantages, future work should focus on expanding the dataset and incorporating additional imaging techniques to enhance diagnostic capabilities further. Additionally, real-world clinical validation is necessary to assess the model's applicability in diverse healthcare settings. While this study presents a promising framework for lung disease classification, continuous improvements and adaptation to evolving medical imaging standards will be essential for its broader implementation.

The study highlights the application of various AI-based approaches in the context of the current lung diseases assessment. It emphasizes the potential of convolutional neural networks (CNNs), a deep learning-based technique combined with SVM method, in automatically detecting and distinguishing features from X-ray images related to different pathologies. The focus of future research could be on distinguishing patients with mild symptoms, which may not be accurately visualized on X-rays.

Conclusion

This work presents a multi-class diseases classification framework based on deep learning and machine learning architectures, which classify lung opacity, pneumonia, and COVID-19 compared to normal cases using X-ray images. The proposed VGG16-SVM model outperforms existing works in terms of accuracy, recall, precision, F1 score, and area under the curve (AUC).

Furthermore, the study suggests that combining two techniques could enhance detection accuracy, especially detect different patterns even before symptoms appear. Also, the Identification of regions of interest (ROI) and severity levels classification using powerful classification models is a potential direction for future exploration.

While X-ray and CT images can serve as initial screening tools for different Coronavirus, lung opacity and pneumonia-datasets, they should be followed by specific treatments and comprehensive examination procedures. The implementation of pertinent measures based on positive samples is essential until specific treatments are developed and complete examination procedures are conducted.

Declarations

Ethics approval and consent to participate: This study was carried out under the principles of the Declaration of Helsinki developed by the World Medical Association and approved by the Human Ethics committee of Bechir Hamza Children's Hospital of Tunis.

All methods were carried out in accordance with relevant guidelines and regulations.

The informed consent was waived by the Human Ethics committee of Children's Hospital of Tunis.

Consent for publication: Not Applicable

Competing interests: The authors declare that they have no conflict of interest.

Funding: No funding

Availability of data and materials: The Chest X-ray images used in this study were obtained from multiple publicly available datasets referenced in [28-31], specifically:

28. Rahman T, Khandakar A, Qiblawey Y, Tahir A, Kiranyaz S, Kashem SB, Islam MT, Maadeed SA, Zughaier SM, Khan MS,

Chowdhury ME. Exploring the effect of image enhancement techniques on COVID-19 detection using chest X-ray images. arXiv. 2020. https://doi.org/10.48550/arXiv.2012.02238

29. Islam MN, Alam MGR, Apon TS, Uddin MZ, Allheeib N, Menshawi A, Hassan MM. Interpretable differential diagnosis of non-COVID viral pneumonia, lung opacity, and COVID-19 using tuned transfer learning and explainable AI. Healthcare. 2023;11(3):410. https://doi.org/10.3390/healthcare11030410

30. Muljo HH, Pardamean B, Purwandari K, Cenggoro TW. Improving lung disease detection by joint learning with COVID-19 radiography database.Commun Math BiolNeurosci. 2022;2022. https://doi.org/10.28919/cmbn/6838

31. Tsai EB, Simpson S, Lungren MP, Hershman M, Roshkovan L, Colak E, Erickson BJ, Shih G, Stein A, Kalpathy-Cramer J, Shen J, Hafez M, John S, Rajiah P, Pogatchnik BP, Mongan J, Altinmakas E, Ranschaert ER, Kitamura FC, ... Wu CC. The RSNA International COVID-19 Open Radiology Database (RICORD). Radiology. 2021;299(1):E204-E213.https://doi.org/10.1148/RADIOL.2021203957

Authorship

ABS, wrote the manuscript and developed the models; YA, SB, and HBR edited manuscript, created the **Figures**, completed data collection clinical guidelines, and clinical evaluation. HT, responsible for the research design. All Authors have contributed to the drafting and the critical revision of the article. The final version approved by all authors.

Acknowledgements

We are deeply grateful to all those who contributed to the success of this research project.

REFERENCES

1. Soffer S, Morgenthau AS, Shimon O, et al. Artificial Intelligence for Interstitial Lung Disease Analysis on Chest Computed Tomography: A Systematic Review. Academic Radiology. 2022;29:S226-S235. doi:10.1016/j.acra.2021.05.014
2. Cookson W, Moffatt M, Rapeport G, Quint J. A Pandemic Lesson for Global Lung Diseases: Exacerbations Are Preventable. Am J Respir Crit Care Med. 2022;205(11):1271-1280. doi:10.1164/rccm.202110-2389ci
3. Doe G, Taylor SJ, Topalovic M, et al. Spirometry services in England post-pandemic and the potential role of AI support software: a qualitative study of challenges and opportunities. Br J Gen Pract. 2023;73(737):e915-e923. doi:10.3399/bjgp.2022.0608
4. Parthasarathy V, Saravanan S. Computer aided diagnosis using Harris Hawks optimizer with deep learning for pneumonia detection on chest X-ray images. Int j inf tecnol. 2024;16(3):1677-1683. doi:10.1007/s41870-023-01700-1
5. Mannepalli DP, Namdeo V. A cad system design based on HybridMultiscale convolutional Mantaray network for pneumonia diagnosis. Multimed Tools Appl. 2022;81(9):12857-12881. doi:10.1007/s11042-022-12547-2
6. Kim S, Rim B, Choi S, Lee A, Min S, Hong M. Deep Learning in Multi-Class Lung Diseases' Classification on Chest X-ray Images. Diagnostics. 2022;12(4):915. doi:10.3390/diagnostics12040915
7. Liu H, Wang L, Nan Y, Jin F, Wang Q, Pu J. SDFN: Segmentation-based deep fusion network for thoracic disease classification in chest X-ray images. Computerized Medical Imaging and Graphics. 2019;75:66-73. doi:10.1016/j.compmedimag.2019.05.005
8. Shen D, Wu G, Suk HI. Deep Learning in Medical Image Analysis. Annu Rev Biomed Eng. 2017;19(1):221-248. doi:10.1146/annurev-bioeng-071516-044442
9. Wang J, Zhu H, Wang SH, Zhang YD. A Review of Deep Learning on Medical Image Analysis. Mobile Netw Appl. 2020;26(1):351-380. doi:10.1007/s11036-020-01672-7
10. Albahli S, Tayyab Rauf H, Arif M, Tabrez Nafis M, Algosaibi A. Identification of Thoracic Diseases by Exploiting Deep Neural Networks. Computers, Materials & Continua. 2021;66(3):3139-3149. doi:10.32604/cmc.2021.014134
11. Chen X, Wang X, Zhang K, et al. Recent advances and clinical applications of deep learning in medical image analysis. Medical Image Analysis. 2022;79:102444. doi:10.1016/j.media.2022.102444
12. Sevi M, AYDIN I. COVID-19 Detection Using Deep Learning Methods. 2020 International Conference on Data Analytics for Business and Industry: Way Towards a Sustainable Economy (ICDABI). Published online October 26, 2020:1-6. doi:10.1109/icdabi51230.2020.9325626
13. Wang D, Mo J, Zhou G, Xu L, Liu Y. An efficient mixture of deep and machine learning models for COVID-19 diagnosis in chest X-ray images. Gwak J, ed. PLoS ONE. 2020;15(11):e0242535. doi:10.1371/journal.pone.0242535
14. Aggarwal R, Sounderajah V, Martin G, et al. Diagnostic accuracy of deep learning in medical imaging: a systematic review and meta-analysis. npj Digit Med. 2021;4(1). doi:10.1038/s41746-021-00438-z
15. Nwankpa CE. Advances in Optimisation Algorithms and Techniques for Deep Learning. Adv sci technol eng syst j. 2020;5(5):563-577. doi:10.25046/aj050570
16. Kalaivani N, Manimaran N, Sophia DrS, D Devi D. Deep Learning Based Lung Cancer Detection and Classification. IOP Conf Ser: Mater Sci Eng. 2020;994(1):012026. doi:10.1088/1757-899x/994/1/012026
17. Ni Q, Sun ZY, Qi L, et al. A deep learning approach to characterize 2019 coronavirus disease (COVID-19) pneumonia in chest CT images. Eur Radiol. 2020;30(12):6517-6527. doi:10.1007/s00330-020-07044-9
18. Xu X, Jiang X, Ma C, et al. A Deep Learning System to Screen Novel Coronavirus Disease 2019 Pneumonia. Engineering. 2020;6(10):1122-1129. doi:10.1016/j.eng.2020.04.010
19. Law BK, Lin LP. Development Of A Deep Learning Model To Classify X-Ray Of Covid-19, Normal And Pneumonia-Affected Patients. 2021 IEEE International Conference on Signal and Image Processing Applications (ICSIPA). Published online September 13, 2021. doi:10.1109/icsipa52582.2021.9576804

20. Liu C, Wang X, Liu C, Sun Q, Peng W. Differentiating novel coronavirus pneumonia from general pneumonia based on machine learning. BioMed Eng OnLine. 2020;19(1). doi:10.1186/s12938-020-00809-9
21. Narin A, Kaya C, Pamuk Z. Automatic detection of coronavirus disease (COVID-19) using X-ray images and deep convolutional neural networks. Pattern Anal Applic. 2021;24(3):1207-1220. doi:10.1007/s10044-021-00984-y
22. Goel G. Real-Time Computed Tomography-based Medical Diagnosis Using Deep Learning [Doctoral dissertation]. Virginia Tech; 2022. http://hdl.handle.net/10919/108853
23. Mann PS, Panchal SD, Singh S, Saggu GS, Gupta K. A hybrid deep convolutional neural network model for improved diagnosis of pneumonia. Neural Comput & Applic. 2023;36(4):1791-1804. doi:10.1007/s00521-023-09147-y
24. Hashmi MF, Katiyar S, Hashmi AW, Keskar AG. Pneumonia detection in chest X-ray images using compound scaled deep learning model. Automatika. 2021;62(3-4):397-406. doi:10.1080/00051144.2021.1973297
25. Malik H, Anees T, Din M, Naeem A. CDC_Net: multi-classification convolutional neural network model for detection of COVID-19, pneumothorax, pneumonia, lung Cancer, and tuberculosis using chest X-rays. Multimed Tools Appl. 2022;82(9):13855-13880. doi:10.1007/s11042-022-13843-7
26. Ayan E, Unver HM. Diagnosis of Pneumonia from Chest X-Ray Images Using Deep Learning. 2019 Scientific Meeting on Electrical-Electronics & Biomedical Engineering and Computer Science (EBBT). Published online April 2019:1-5. doi:10.1109/ebbt.2019.8741582
27. El Asnaoui K, Chawki Y, Idri A. Automated Methods for Detection and Classification Pneumonia Based on X-Ray Images Using Deep Learning. Studies in Big Data. Published online 2021:257-284. doi:10.1007/978-3-030-74575-2_14
28. Rahman T, Khandakar A, Qiblawey Y, et al. Exploring the effect of image enhancement techniques on COVID-19 detection using chest X-ray images. Computers in Biology and Medicine. 2021;132:104319. doi:10.1016/j.compbiomed.2021.104319
29. Islam MdN, Alam MdGR, Apon TS, et al. Interpretable Differential Diagnosis of Non-COVID Viral Pneumonia, Lung Opacity and COVID-19 Using Tuned Transfer Learning and Explainable AI. Healthcare. 2023;11(3):410. doi:10.3390/healthcare11030410
30. Improving lung disease detection by joint learning with COVID-19 radiography database. Commun Math Biol Neurosci. Published online 2022. doi:10.28919/cmbn/6838
31. Tsai EB, Simpson S, Lungren MP, et al. The RSNA International COVID-19 Open Radiology Database (RICORD). Radiology. 2021;299(1):E204-E213. doi:10.1148/radiol.2021203957
32. Ibrahim AU, Ozsoz M, Serte S, Al-Turjman F, Yakoi PS. Pneumonia Classification Using Deep Learning from Chest X-ray Images During COVID-19. Cogn Comput. 2021;16(4):1589-1601. doi:10.1007/s12559-020-09787-5
33. Anwar SM, Majid M, Qayyum A, Awais M, Alnowami M, Khan MK. Medical Image Analysis using Convolutional Neural Networks: A Review. J Med Syst. 2018;42(11). doi:10.1007/s10916-018-1088-1
34. Jeyaraj PR, Samuel Nadar ER. Computer-assisted medical image classification for early diagnosis of oral cancer employing deep learning algorithm. J Cancer Res Clin Oncol. 2019;145(4):829-837. doi:10.1007/s00432-018-02834-7
35. Kumar A, Kim J, Lyndon D, Fulham M, Feng D. An Ensemble of Fine-Tuned Convolutional Neural Networks for Medical Image Classification. IEEE J Biomed Health Inform. 2017;21(1):31-40. doi:10.1109/jbhi.2016.2635663
36. Rahul, Goyal B. Gaussian Filtering based Image Integration for Improved Disease Diagnosis and Treatment Planning. 2021 9th International Conference on Reliability, Infocom Technologies and Optimization (Trends and Future Directions) (ICRITO). Published online September 3, 2021:1-6. doi:10.1109/icrito51393.2021.9596278
37. M. A, Govindharaju K, A. J, Mohan S, Ahmadian A, Ciano T. A hybrid learning approach for the stage-wise classification and prediction of <scp>COVID</scp>-19 X-ray images. Expert Systems. 2021;39(4). doi:10.1111/exsy.12884
38. Jiang ZP, Liu YY, Shao ZE, Huang KW. An Improved VGG16 Model for Pneumonia Image Classification. Applied Sciences. 2021;11(23):11185. doi:10.3390/app112311185
39. Panja A, Christy JJ, Abdul QM. An Approach to Skin Cancer Detection using Keras and Tensorflow. J Phys: Conf Ser. 2021;1911(1):012032. doi:10.1088/1742-6596/1911/1/012032
40. Yadavendra, Chand S. Pneumonia lung opacity detection and segmentation in chest x-rays by using transfer learning of the Mask R-CNN. 2021 7th International Conference on Advanced Computing and Communication Systems (ICACCS). Published online March 19, 2021:1035-1040. doi:10.1109/icaccs51430.2021.9441864
41. Ibrokhimov B, Kang JY. Deep Learning Model for COVID-19-Infected Pneumonia Diagnosis Using Chest Radiography Images. BioMedInformatics. 2022;2(4):654-670. doi:10.3390/biomedinformatics2040043
42. Monshi MMA, Poon J, Chung V, Monshi FM. CovidXrayNet: Optimizing data augmentation and CNN hyperparameters for improved COVID-19 detection from CXR. Computers in Biology and Medicine. 2021;133:104375. doi:10.1016/j.compbiomed.2021.104375
43. Sandler M, Howard A, Zhu M, Zhmoginov A, Chen LC. MobileNetV2: Inverted Residuals and Linear Bottlenecks. 2018 IEEE/CVF Conference on Computer Vision and Pattern Recognition. Published online June 2018:4510-4520. doi:10.1109/cvpr.2018.00474
44. Rajpal S, Lakhyani N, Singh AK, Kohli R, Kumar N. Using handpicked features in conjunction with ResNet-50 for improved detection of COVID-19 from chest X-ray images. Chaos, Solitons & Fractals. 2021;145:110749. doi:10.1016/j.chaos.2021.110749
45. Hamlili FZ, Beladgham M, Khelifi M, Bouida A. Transfer learning with Resnet-50 for detecting COVID-19 in chest X-ray images. IJEECS. 2022;25(3):1458. doi:10.11591/ijeecs.v25.i3.pp1458-1468
46. Baltazar LR, Manzanillo MG, Gaudillo J, et al. Artificial intelligence on COVID-19 pneumonia detection using chest xray images. Zhang J, ed. PLoS ONE. 2021;16(10):e0257884. doi:10.1371/journal.pone.0257884
47. Chollet F. Xception: Deep Learning with Depthwise Separable Convolutions. 2017 IEEE Conference on Computer Vision and Pattern Recognition (CVPR). Published online July 2017:1800-1807. doi:10.1109/cvpr.2017.195
48. Showkat S, Qureshi S. Efficacy of Transfer Learning-based ResNet models in Chest X-ray image classification for detecting COVID-19 Pneumonia. Chemometrics and Intelligent Laboratory Systems. 2022;224:104534. doi:10.1016/j.chemolab.2022.104534
49. Javad Zadeh Barzaki MA, Abdollahi J, Negaresh M, et al. Using Deep Learning for Classification of Lung Cancer on CT Images in Ardabil Province : Classification of Lung Cancer using Xception. 2023 13th International Conference on Computer and Knowledge Engineering (ICCKE). Published online November 1, 2023:375-382. doi:10.1109/iccke60553.2023.10326262
50. Badawy M, Almars AM, Balaha HM, Shehata M, Qaraad M, Elhosseini M. A two-stage renal disease classification based on transfer learning with hyperparameters optimization. Front Med. 2023;10. doi:10.3389/fmed.2023.1106717

51. Houssein EH, Mohamed O, Abdel Samee N, et al. Using deep DenseNet with cyclical learning rate to classify leukocytes for leukemia identification. Front Oncol. 2023;13. doi:10.3389/fonc.2023.1230434

52. Tun NL, Gavrilov A, Tun NM, Trieu DM, Aung H. Remote Sensing Data Classification Using A Hybrid Pre-Trained VGG16 CNN- SVM Classifier. 2021 IEEE Conference of Russian Young Researchers in Electrical and Electronic Engineering (ElConRus). Published online January 26, 2021:2171-2175. doi:10.1109/elconrus51938.2021.9396706

53. Bhatt H, Shah M. A Convolutional Neural Network ensemble model for Pneumonia Detection using chest X-ray images. Healthcare Analytics. 2023;3:100176. doi:10.1016/j.health.2023.100176

54. Ho TK, Gwak J. Multiple Feature Integration for Classification of Thoracic Disease in Chest Radiography. Applied Sciences. 2019;9(19):4130. doi:10.3390/app9194130

55. Ben Slama A, Sahli H, Amri Y, Labidi S. V-NET-VGG16: Hybrid deep learning architecture for optimal segmentation and classification of multi-differentiated liver tumors. Intelligence-Based Medicine. 2025;11:100210. doi:10.1016/j.ibmed.2025.100210

56. Amri Y, Ben Slama A, Mbarki Z, Selmi R, Trabelsi H. Automatic glioma segmentation based on efficient U-net model using MRI images. Intelligence-Based Medicine. 2025;11:100216. doi:10.1016/j.ibmed.2025.100216